3rd Inter. Conf. Virol., Cairo Univ. Center, Nov. 24-25, 2010
Egyptian J. Virol., SP. Issue, 465-484, 2010

PARTIALLY NUCLEOTIDE SEQUENCE AND SECONDARY STRUCTURE OF *CHRYSANTHEMUM STUNT VIROID* EGYPTIAN ISOLATE FROM INFECTED *CHRYSANTHEMUM* PLANTS

[31]

El-Dougdoug[1], Kh.A.; Rezk[2], A.A.; Dawoud[2], Rehab A. and Sofy[3]*, A.R.

Chrysanthemum *stunt viroid* Egyptian isolate (CSVd-EG) was isolated from infected *Chrysanthemum* plants. It is a member of *Pospiviroidae*. In order to study the structure of CSVd-EG, it was reverse transcribed in total RNA from infected leaves and then amplified by polymerase chain reaction (PCR) using *Pospiviroid*-CCR specific primers. Purified gel RT-PCR product (~199) was cloned into the PCR® II - TOPO® vector then it was sequenced. Partial sequence 199 bp of CSVd-EG is almost identical to that of the prototype 199 bp Canada and USA isolates of CSVd with 96% homology. The sequence of CSVd-EG can be arranged into viroid specific rod like structure. CSVd-EG differ from the prototype isolates Canada and USA at sites occur in regions corresponding to the conserved, variable and right terminal domains which are believed to control viroid pathogencity. Finally, this constitutes the first isolation and identification of CSVd from diseased *Chrysanthemum* plants in Egypt

Keywords: *Chrysanthemum*, CSVd-EG, viroid, RT-PCR, cloning, sequence, Egypt

[1]Virology Lab., Agric. Microbiology Department, Faculty of Agriculture, Ain Shams University, 11241 Cairo, Egypt.
[2]Plant Virus and Phytoplasma Research Section, Plant Pathology Institute, Agriculture Research Center, Giza, Egypt.
[3]Botany and Microbiology Department, Faculty of Science, Al-Azhar University, 11884 Nasr City, Cairo, Egypt.
*ahmd_sofy@yahoo.com

INTRODUCTION

Chrysanthemum stunt viroid (CSVd) is the type member of the genus *Pospiviroid* (family *Pospiviroidae*). It is a single stranded circular RNA molecular about 348-356 nt in length and non capsidated (**Diener, 1987**). It consists of five structural domains, central conserved (CCR), pathogencity (P), variable (V), right and left terminal domains (T1 and T2). It has a high degree of internal sequence complementary and complex-secondary structure. The secondary structure during thermal denaturation undergo several structural transitions from rod-like to the single stranded circle without any intramolecular base pairing (**Loss *et al.*, 1991**). In a highly cooperative main transition, all base pairs of the native structure, are disrupted and particularly stable hairpins newly formed (HpI, HpII and HpIII). Secondary structure almost become an identification criterion for viroids (**Bussiere *et al.*, 1996**). In addition, **Mathews and Turner (2006)** observed that the best algorithms for predicting the secondary structure of a single RNA molecule is finding the minimum free energy (mfe) of the secondary structure which based on dynamic programming algorithms. **Serra *et al.* (1995)** assume that the total free energy, of a given secondary structure for a molecule, is the sum of independent contributions of adjacent, or stacked, base pairs in stems (which tend to stabilize the structure) and loops (which tend to destabilize the structure).

This work aims at carrying out the nucleotide sequence and minimum free energy of secondary structure of CSVd from diseased *Chrysanthemum*. It is reverse transcriped and then amplified from total RNA extracts of infected tissues. This record is the first time in Egypt.

MATERIALS & METHODS

Plant samples

Leaf samples (*Chrysanthemum morifolium* cv. white) were collected from plants grown at greenhouse, Horticulture Dept., Fac., of Agric., Ain Shams Univ. at autumn season. These plants have shown viroid-like symptoms (Fig. 1).

Total RNA extraction and RT-PCR

Total RNA were extracted from diseased and healthy *C. morifolium* leaves using the EZ-10 Spin Column Total RNA Minipreps

Super Kit (BIO BASIC INC). One pair of degenerate *Pospiviroid* primers was used to generate overlapping cDNA. *Pospiviroid* complementary primer (5'-ATTAATCCCCGGGGAAACCTG GAG-3') and homologous primer (5'-AGCTTCAGTTGTTTCCACCGGGT-3') were designed to amplify partial sequence of CSVd (**Bostan *et al.*, 2004**). The cDNA synthesis and PCR amplification were done according to methodology of **Bostan *et al.* (2004)**.

Cloning and sequence analysis

The amplified cDNA products were purified using QIAquick Gel Extraction kit (Qiagene). The resulting fragments were cloned into PCR® II - TOPO® vector (Invitrogen, Carlsbad, CA, USA) using *Eco*RI and transformed into *E. coli* DH5α. Selected clones were sequenced using an automated DNA sequencer (ABI PRISMTM 3730XL DNA Analyzer) and analyzed by FinchTV™ version 1.4.0 software.

Sequencing analysis and determination of secondary structures

Sequences of eight CSVd in the GenBank (DQ406591 Canada, AJ001851 USA, AB279771 Japan, X16409 Germany, AF394453 Korea, AJ000046 Hungary, DQ094398 Netherlands and AJ585258 India) were aligned with the Egyptian CSVd sequence deposited in the GenBank database (Accession number: GQ229575) using ClustalW (Ver.1.74) program (**Thompson *et al.*, 1994**). The nucleotide distances were estimated considering alignment gaps using the Jukes and Cantor's method (**Jukes and Cantor, 1969**) for correction of superimposed substitutions using the Molecular Evolutionary Genetics Analysis (MEGA) software (Ver. 4.0) (**Tamura *et al.*, 2007**). Neighbour Joining (NJ) was implemented through MEGA 4.0 software, and bootstrap analysis (1000 replicates) was performed to assess the reliability of the constructed phylogenetic tree. Secondary structures were obtained with the MFOLD program (circular version) of the GCG package (**Zuker, 1989**) at 37°C.

RESULTS

The diseased *Chrysanthemum* plants showing mottling symptoms on leaves which are narrow and stem is stunting (**Figure 1**). Stunted growth is recognized between

healthy and diseased plants at the same age grown side by side. Upper leaves on flowering stems are much smaller than corresponding leaves on healthy plants. Lower leaves of some varieties are curled upward sharply at the margins (**Figure 1**).

The RNA template of CSVd Egyptian isolate was reverse transcribed by MMLV reverse transcriptase. The resulting cDNA was amplified by PCR using universal *Pospiviroid* primers specific for CCR. The PCR product was analyzed on agarose gel 1.5% electrophoresis. The expected size of amplified CSVd cDNA was approximately ~199 bp. While the healthy leaves were not amplified by RT-PCR (**Figure 2**).

The cloned amplified fragment of PCR products were ligated directly into PCR® II - TOPO® vector. The recombinant plasmids were introduced into *E. coli* strain DH5α as described by manufacturer's instructions. DNA was prepared from selected white colonies, digested with *Eco*RI and fractionated on agarose gel using 1Kb DNA ladder. The nucleotide sequence of PCR-amplified CSVd-RNA was determined directly from partial length overlapping PCR products and confirmed by CSVd clone. CSVd consist of 199 nucleotide (**Figure 2**).

Genetic diversity between CSVd-EG isolate and 8 reported CSVd sequences in GenBank from Canada (Accession No. DQ406591), USA (Accession No. AJ001851), Japan (Accession No. AB279771), Germany (Accession No. X16409), Korea (Accession No. AF394453), Hungary (Accession No. AJ000046), Netherlands (Accession No. DQ094398) and India (Accession No. AJ585258). All of these sequences were multiple-aligned at the same partial sequence of CSVd-EG using ClustalW program with minor manual adjustments, resulting in 199 positions including the gaps (**Figure 3**). A total of 10 variable sites were found in CSVd, 2 of which were parsimoniously informative nucleotide sites and 8 of which were singleton sites. A phylogenetic tree was constructed for showing the clustering relationship among CSVd populations. It was generated using the Neighbour-Joining method and bootstrap analysis of 1000 repetitions, produced two major groups (**Figure 4**). Statistical analysis of alignment sequence of CSVd-EG with two geographically distant CSVd strains available from

GenBank (**Table 1**) revealed that molecular characters CSVd-EG strain, the molecular weight (63.77 KDa); base composition (A: 42, C: 59, G: 49, U: 49, A/U: 91 and C/G: 108); frequencies nucleotides (A: 21.2, C: 29.6, G: 29.6, U: 24.6, A/U: 45.7 and C/G: 54.3) (**Figure 3 and Table 1**).

The sequence can be arranged into the rod-like secondary structure as characteristic of viroid with lowest free energy of -67.10 K.cal/mol at 37°C (**Figure 5**). Also, CSVd-EG has Y-shaped structure composed of alternating single end double-stranded regions with lowest free energy of -65.40 K.cal/mol at 37°C (**Figure 6**). CSVd-EG has 97% and 96.5% homologous with 199 nucleotide of Canada and USA strains respectively and differs at 8 sites, as compared with and related to the type strains (U_2, U_3, A_4, C_{48}, A_{49}, G_{102}, U_{104} and U_{132}) (**Figure 7**). Three out of eight changes occur in the center conserved domain (CCR). Three more changes in variable domain (V) and two more in the right terminal domain (T2) (**Figures 5 and 7**). Most of the changes among CSVd-Egypt, CSVd-Canada and CSVd-USA occur in regions corresponding to CCR, V and T2 domains which are for variation in CSVd strains (**Figures 7 & 8**). The nucleotide sequence of CSVd-EG also confirm our previous findings which suggested that CSVd-EG is a member of genus *Pospiviroid* as indicated by PCR amplification using universal *Pospiviroid* primers.

CSVd, generally, has rod-like structure, that was characterized by a series of double helical sections and internal loops, as average of each helical sequence of four to five base pairs is followed by a defect in the form of an internal loop of two bases. Quantitative thermodynamic, kinetic studies of their thermal denaturation; number of helix nucleation structures and free energy in rod like shape of CSVd-EG (External loops: 1 with $-\Delta G=$ 1.10, Bulge loops: 4 with $\Delta G=$ 8.2, Interior loops: 8 with $\Delta G=$ 19.6, Hairpin loops: 1 with $\Delta G=$ 3.6 and stacks: 51 with $-\Delta G=$ 97.4) were used for recognition. Moreover, Y-shape of CSVd-EG (External loops: 1 with $-\Delta G=$ 2.5, Bulges: 4 with $\Delta G=$ 8.2, Interior loops: 8 with $\Delta G=$ 18.3, Hairpin loops: 3 with $\Delta G=$ 7.7 and stacks: 50 with $-\Delta G=$ 97.1) were used as more characteristics to compare with

CSVd-Canada and CSVd-USA strains (**Table 2**). ΔG°37 (Gibbs free energy) of stalking pairs, interior, hairpin and bulge loops depend on predicted free energy values (Kcal/mol at 37°C). It was observed that base pairs lead to free energy < 0 while bulges and loops lead to free energies > 0. Consequently total free energy of CSVd Egyptian isolate was -67.10°C Kcal/mol and -65.40 K.cal/mol at 37°C for rod-like and Y-like shape structures respectively (**Table 3**). The calculation of the free energy of a given base-pairing scheme is carried out, in the way that the structure is built up starting from the completely coiled-viroid strand, to forming, step by step, base pairing. Whenever a base pair is formed, next to already existing base pairs, it closes a loop of unpaired nucleotides. Therefore, following stability parameters, Gibbs free energy (ΔG) -67.10°C & -65.40°C Kcal/mol; reaction enthalpy (ΔH) -593.50 & -617.50 Kcal/mol; reaction entropy (ΔS) -1697.2 & -1780.1 Kcal/mol and melting temperature (Tm) 76.5°C & 73.7°C in rod-like shape and Y-like shape respectively are listed in **Table (3)** and **Figure (5 and 6).**

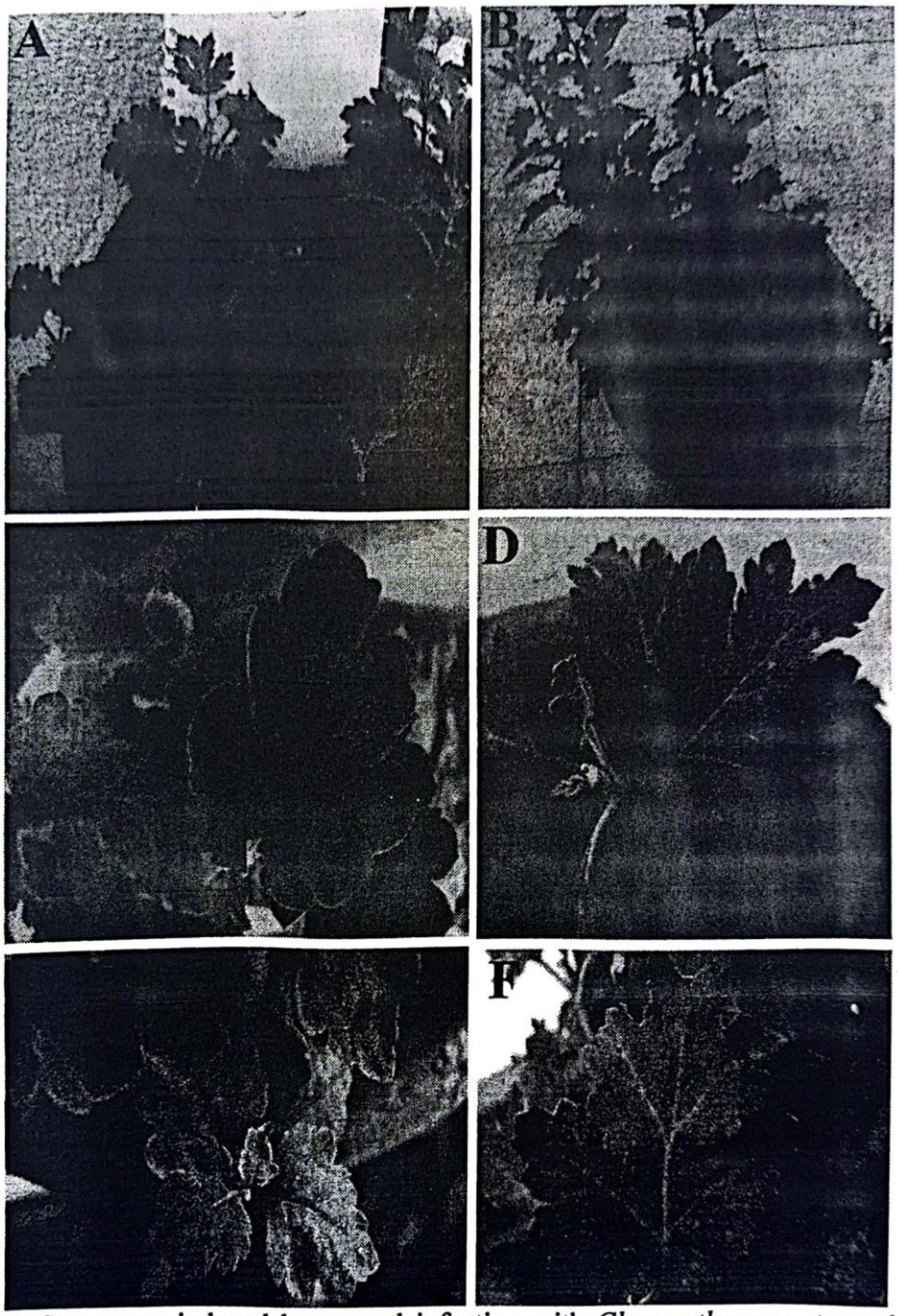

Figure 1. Symptoms induced by natural infection with *Chrysanthemum stunt viroid* on chrysanthemum plants. (A) Healthy plant, (B) Healthy and diseased plants of the same age are grown side by side showing stunted growth, (C & D) Yellow spots, (E) Mottling, (F) Vein clearing.

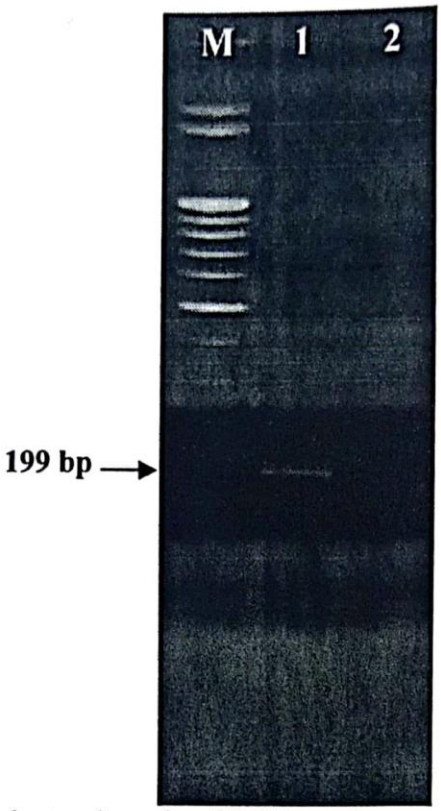

Figure 2. Agarose gel electrophoresis of PCR product produced from *Chrysanthemum stunt viroid* (CSVd) Egyptian isolate (lane 1) and healthy plant (lane 2). M: DNA size marker (100 bp ladder). Arrow indicates the location of the amplification products.

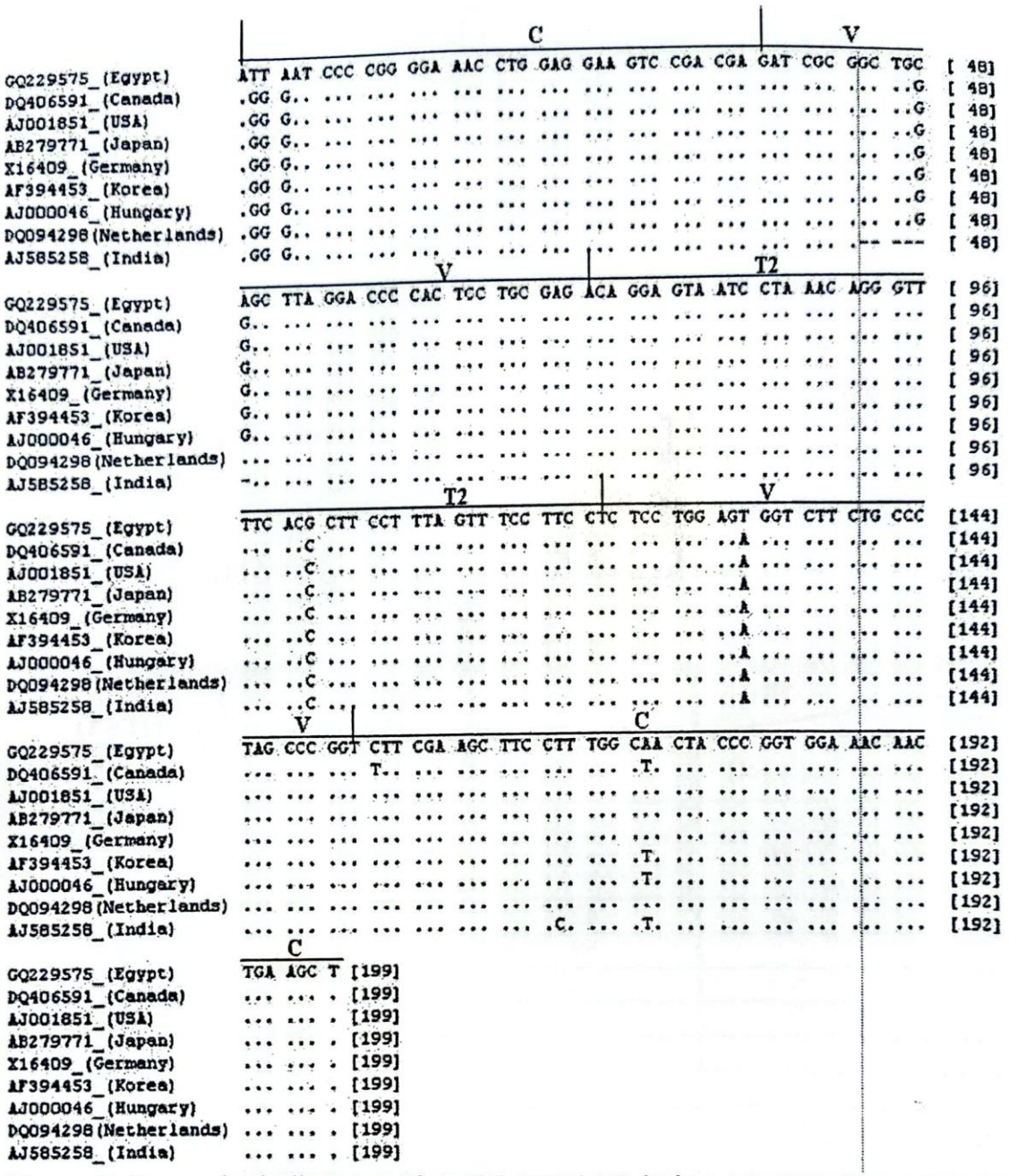

Figure 3. Summarized alignment of partial CSVd-EG isolate sequence (Accession no. GQ229575) and 8 CSVd sequences published in GenBank using clustalw program resulting in 199 positions including the gaps. Domains: C (central), V (variable) and T2 (terminal right) **(Keese and Symons, 1985)**.

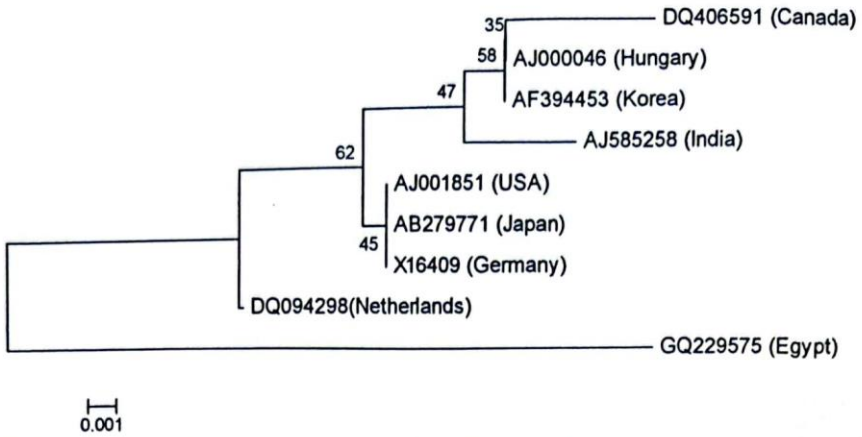

Figure 4. Neighbour-joining tree of CSVd-EG isolate (Accession no. GQ229575) and 8 strains of CSVd published in GenBank. Numbers represent bootstrap percentage values based on 1000 replicates.

Table 1. Base composition and sequence homology domains of CSVd-EG, CSVd-Canada and CSVd-USA

Strains / Comparison	GQ229575 (Egypt)	DQ094298 (Canada)	AJ001851 (USA)
Length on nucleic acids (nt)	199	199	199
M.W. (kDa)	63,77	63,89	63,90
No. of nucleotides base composition			
A	42	42	41
C	59	59	59
G	49	52	53
U	49	46	46
A/U	91	88	87
C/G	108	111	112
Frequencies nucleotides			
A	21.2	21.2	20.6
C	29.6	29.6	29.6
G	24.6	26.1	26.6
U	24.6	23.1	23.2
A/U	45.7	44.2	43.7
C/G	54.3	55.8	56.3

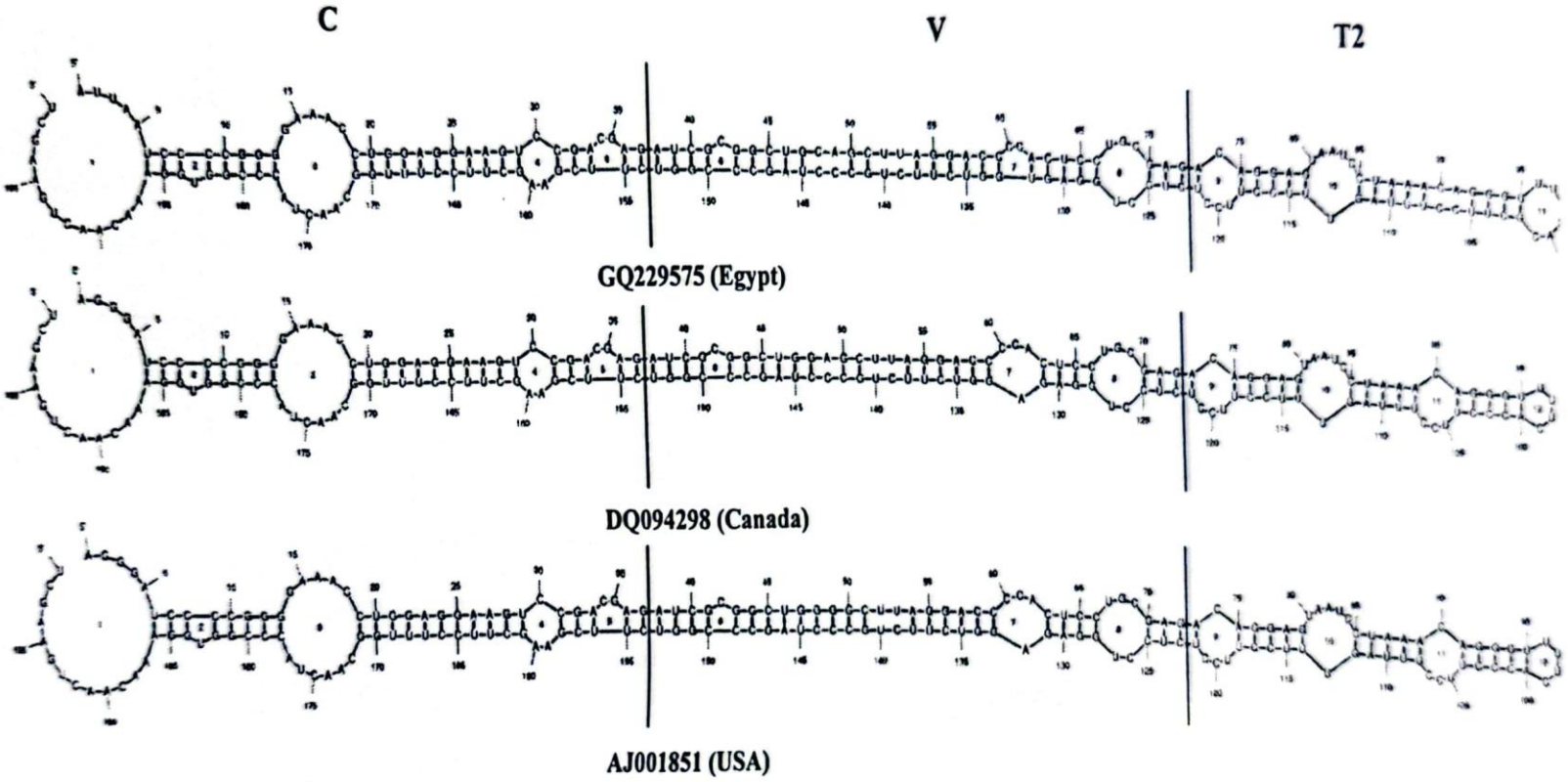

Figure 5. The secondary structure of partial RNA CSVd-EG, CSVd-Canada and CSVd-USA isolates are rod-shaped structure. Domains: C (central), V (variable) and T2 (terminal right) **(Keese and Symons, 1985).**

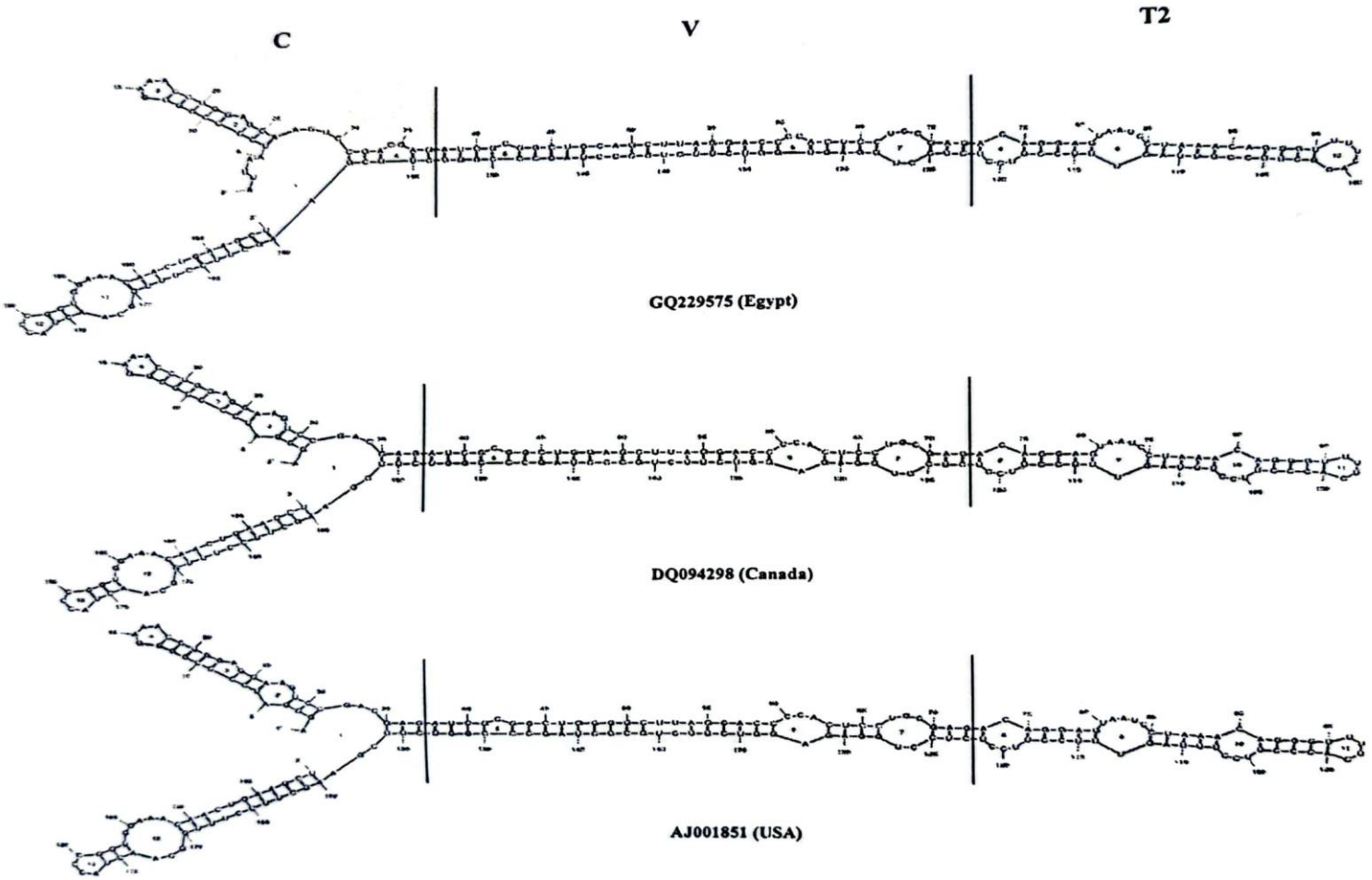

Figure 6. The secondary structure of partial RNA CSVd-EG, CSVd-Canada and CSVd-USA isolates are Y-shaped structure. Domains: C (central), V (variable) and T2 (terminal right) (**Keese and Symons, 1985**).

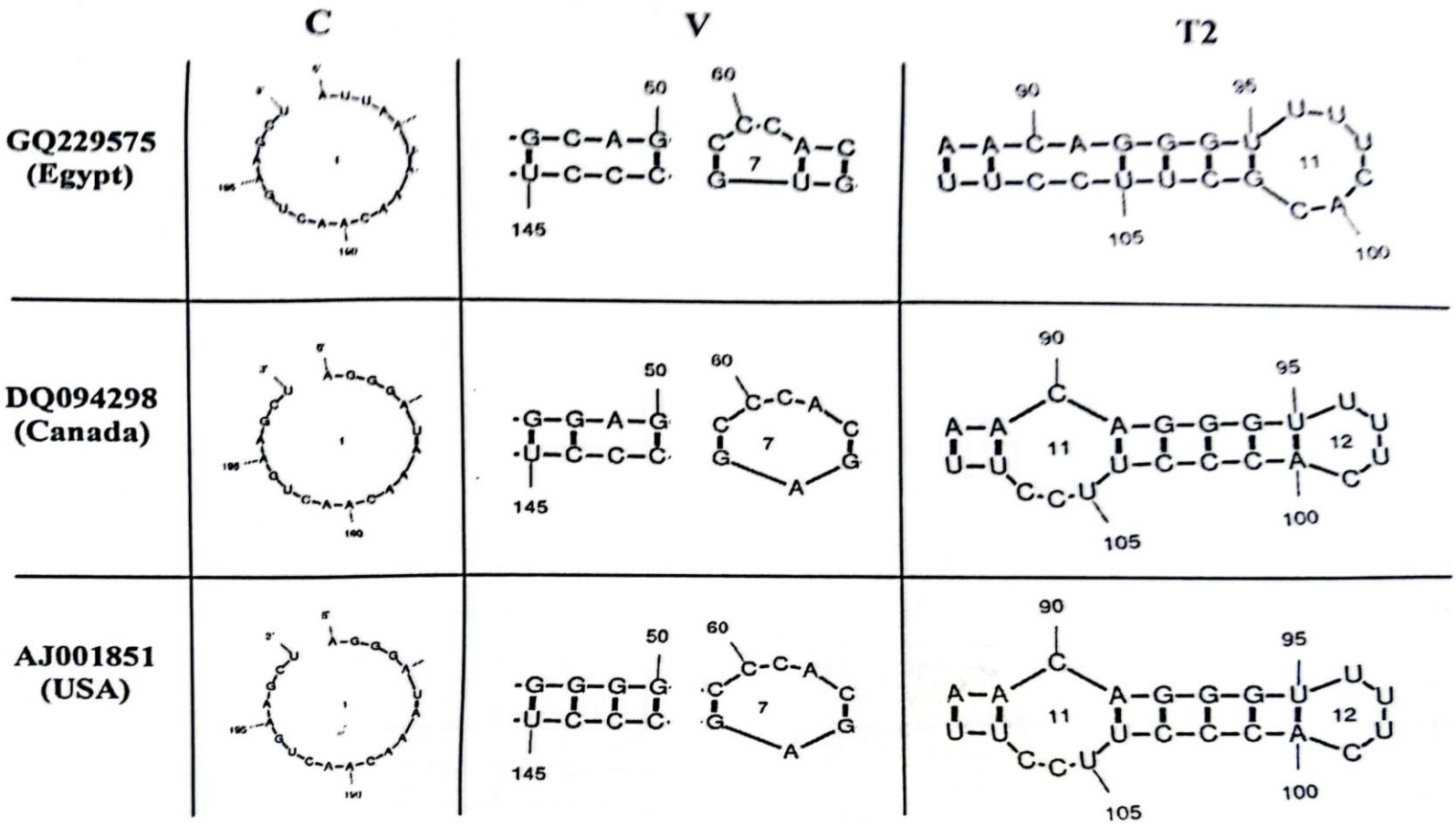

Figure 7. Sequence homology between domains of rod-shaped secondary structure for CSVd-EG, CSVd-Canada and CSVd-USA isolates.

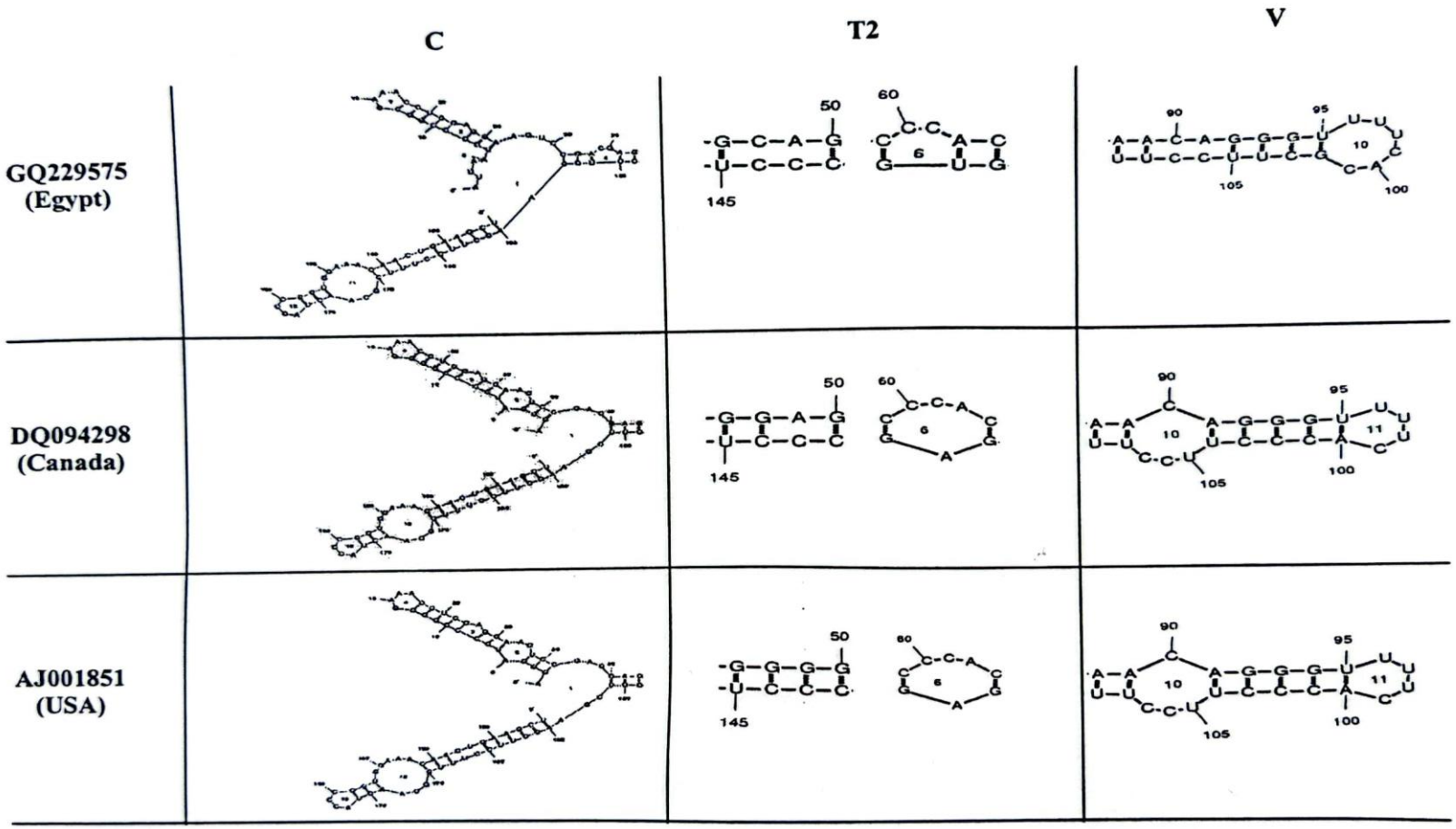

Figure 8. Sequence homology between domains of Y-shaped secondary structure for CSVd-EG, CSVd-Canada and CSVd-USA isolates.

Table 2. Number of helix nucleation structures and free energy of three CSVd strains

Isolates	Rod-like shape									
	Helix nucleation									
	External loops		Bulge loops		Interior loops		Hairpin loops		Stacks	
	No.	$-\Delta G_{37°C}$	No.	$-\Delta G_{37°C}$	No.	$-\Delta G_{37°C}$	No.	$-\Delta G_{37°C}$	No.	$-\Delta G_{37°C}$
GQ229575 (Egypt)	1	1.10	4	8.2	8	19.6	1	3.60	51	97.4
DQ094298 (Canada)	1	1.10	3	5.1	9	21.6	1	4.30	52	102.4
AJ001851 (USA)	1	1.10	3	5.1	8	20.8	1	4.30	54	108.2
	Y-shape									
	Helix nucleation									
	External loops		Bulge loops		Interior loops		Hairpin loops		Stacks	
	No.	$-\Delta G_{37°C}$	No.	$-\Delta G_{37°C}$	No.	$-\Delta G_{37°C}$	No.	$-\Delta G_{37°C}$	No.	$-\Delta G_{37°C}$
GQ229575 (Egypt)	1	2.50	4	8.2	8	18.3	3	7.7	50	97.1
DQ094298 (Canada)	1	2.90	2	2	10	22	3	8.4	52	103.2
AJ001851 (USA)	1	2.90	2	2	9	21.2	3	8.4	54	109

Table 3. Stability parameters of rod and Y-like shapes of three CSVd strains

Isolates	Structure							
	Rod-like shape				Y-shape			
	$-\Delta G_{37°C}$ (kcal/mol)	$-\Delta H$ (kcal/mol)	$-\Delta S$ (cal/mol·K)	Tm (°C)	$-\Delta G_{37°C}$ (kcal/mol)	$-\Delta H$ (kcal/mol)	$-\Delta S$ (cal/mol·K)	Tm (°C)
GQ229575 (Egypt)	67.10	593.50	1697.2	76.5	65.40	617.50	1780.1	73.7
DQ094298 (Canada)	72.50	608.60	1728.5	78.9	73.70	642.50	1833.9	77.1
AJ001851 (USA)	79.10	633.00	1785.9	81.2	80.30	666.90	1891.3	79.4

$-\Delta G_{37°C}$: Free energy (Gibbs free energy) at 37°C **$-\Delta H$** : Reaction enthalpy

$-\Delta S$: Reaction entropy

DISCUSSION

Chrysanthemum stunt was first recognized in the US in 1945 (**Hadidi *et al.*, 2003**), and the epidemic caused by CSVd in cultivated chrysanthemums developed during 1945–1947 was recorded (**Brierley and Smith, 1949**). The disease spread rapidly, first to Canada and in the 1950s to all areas of the world where chrysanthemums are grown, probably through the international transport of cuttings (**Lawson, 1987**). In spite of, the worldwide distribution of CSVd in *Chrysanthemum* and its effect on the quality of the plant, there has been no research on CSVd in Egypt. CSVd Egyptian isolate (CSVd-EG) was identified in field-grown chrysanthemums based on symptomatology, RT-PCR, nucleotide sequence determination and bioinformatics analysis. The most common effects are reduction in plant size to one-half to two-thirds, poor root development as well as leaf discoloration. Fresh weight of the flowers can be reduced by 65% (**Horst *et al.*, 1977**). Stunted growth is best recognized when healthy and diseased plants of the same age are grown side by side (**Figure 1**). Leaves are often thinner and paler green color and they are much smaller (**Figure 1**) (**Brierley and Smith, 1951**). Symptom of chlorosis of leaves and mottle on leaves was uncommon, although yellowing of young leaves of chrysanthemum was previously reported by **Dusi *et al.* (1990)**. Further characterization of the caused viroid has been used as follow: A) total RNA extraction for a reverse transcription polymerase chain reaction (RT-PCR) system according to **Bostan et *al.* (2004)** who used RT-PCR primer pair for the detection of *Pospiviroid*. The expected size of amplicon was approximately 199 bp (**Figure 2**) by using generate *Pospiviroid* which is targeted to CCR of the viroid genome. These primers have been selected to allow amplification of all isolates belongs to species and it could be potentially discriminated as variants or strains within a viroid species (**Bostan et *al.* 2004**). B) chromatogram was generated using universal primer for *Pospiviroid*. C) the partial nucleotide sequence of CSVd-EG isolate was deposited in the GenBank database (Accession number: GQ229575) (**Figure 3**). Pairwise comparisons of CSVd-EG with eight

geographically distinct CSVd isolates available from GenBank revealed high sequence identity (96%) (**Nie *et al.*, 2005**). D) the minimum free energy of a secondary structure for CSVd-EG-RNA was determined from its primary sequence (**Figure 3**) by summing the energy contribution of all base pairs, interior loops, hairpin loop, bulge loops and external loop at 37°C (**Figures 5 and 6**) by MFOLD analysis at 37°C (**Diener, 1987**). E) CSVd as rod-like structures has been characterized by a series of double helical sections and internal loops. The partial CSVd-EG sequence appeared to fold into a rod-like and Y-shape structures with the minimum free energy -67.10 and -65.40 K.cal/mol respectively. **Serra *et al.* (1995)** mentioned free energy models assume that, the total free energy of a given secondary structure, is the sum of independent contributions of adjacent, or stacked, base pairs in stems (which tend to stabilize the structure) and of loops (which tend to destabilize the structure). The secondary structure model of CSVd proposed on the basis of its known nucleotide sequence in the model (Accession number: GQ229575). The primary sequence has been arranged to maximize the number of base pair as well as to reflect the location of sites of preferential nuclease cleavage and the sensitivity of cytidine residues to modification by sodium bisulfite (**Bussiere *et al.*, 1996**). According to this model, total of 199 base pairs (guanine-cytosine, adenine-uracil and guanine-uracil pairs) are involved. *Chrysanthemum stunt viroid* Egyptian isolate (CSVd-EG) is most partially related to ChSVd showing 96% overall sequence homology. It is extensive but not complete homology between CSVd-EG and CSVd-Canada and CSVd-USA strains as well as the difference in symptoms expression of the chrysanthemum mottling disease (**Nie *et al.*, 2005**). Besides homology with CSVd-Canada and CSVd-USA, contains several regions of sequence and structural homology with other CSVd-like viroids and is consistent with the domain model proposed by **Hadidi *et al.* (2003); Nie *et al.* (2005)**. Homologous domains include the central conserved regions (C) with the common uridine bulged helix. In contrast with other viroids, the part of the viroid molecule is most highly conserved between CSVd-EG and CSVd corresponds to the most variable domain (V) in the

rest of PSTVd-like viroids. One possibility is that the V domain of CSVd contains sequence that is essential for the partial sequence duplications that is postulated to arise *de novo* during infection of *Chrysanthemum* plants by CSVd (**Hadidi *et al.*, 2003**). The boundaries of these dublications occur in the V domain and at the middle of the loop of the T2 domain of CSVd.

Based on a combination of results obtained by the RT-PCR, sequence, and bioinformatics analysis, it is concluded that the viroid isolated from diseased *Chrysanthemum* plants resembles CSVd in all essential aspects and can, therefore, be considered as different isolate of this viroid. This is the first time that the viroid has been isolated from a naturally infected *Chrysanthemum* plant in Egypt.

REFERENCES

1. **Bostan, H., Nie, X., and Singh, R.P. (2004).** An RT-PCR primer pair for the detection of *Pospiviroid* and its application in surveying ornamental plants for viroids. *Journal of Virological Methods* **116:** 189-193.
2. **Brierley, P. and Smith, F.F. (1949).** Evidence points to virus as cause of chrysanthemum stunt. Florists' Review 103: 36-37.
3. **Brierley, P., and Smith, F.F. (1951).** Chrysanthemum stunt. Control measures effective against virus in florists' crops. Florists' Review 107: 27-30.
4. **Bussiere, F.; D. Lafontaine; J. P. Perreaut (1996).** Compilation and analysis of viroid and viroid-Like RNA sequences. *Nucleic acids research.* 24(10): 1793-1798.
5. **Diener, T.O. (1987).** The viroids. Plenum Press, New York, USA, 339 pp.
6. **Dusi, A. N., Fonseca, M. E. N. and Avila, A. C. (1990).** Occurrence of a viroid in chrysanthemum in Brazil. Plant Pathol. 39: 636-637.
7. **Hadidi, A., Flores, R., Randles, J.W., and Semancik, J.S. (2003).** Viroids. Casiro, Australia 370 pp.
8. **Horst, R.K., Langhans, R.W., and Smith, S.H. (1977).** Effects of chrysanthemum stunt, chlorotic mottle, aspermy and mosaic on flowering and rooting of chrysanthemums. Phytopathology 67: 9-14.

9. **Jukes, T.H., and Cantor, C.R. (1969).** Evolution of protein molecules. In: Munro HN (ed) Mammalian Protein Metabolism. New York, Academic Press, pp 21–132.
10. **Keese, P., and Symons, R.H. (1985).** Domains in viroids: Evidence of intermolecular RNA rearrangements and their contribution to viroid evolution. *Proc. Natl. Acad. Sci. USA*, **82**:4582–4586.
11. **Lawson, R.H. (1987).** Chrysanthemum stunt. Pages 247-259 in: The viroids. T.O. Diener, ed. Plenum Press: New York and London.
12. **Loss, P.; M. Schmitz; G. Steger and D. Riesner (1991).** Formation of a thermodynamically metastable structure containing hairpin II is critical for infectivity of *potato spindle tuber viroid* RNA. *The EMBO J. Vol.* 10(3): 719-727.
13. **Mathews; H. D. and D. H. Turner (2006).** Prediction of RNA secondary structure by free energy minimization. *Current Opinion in Structural Biology*. 16 270-278.
14. **Nie, X., Singh, R.P., and Bostan, H. (2005).** Molecular cloning, secondary structure, and phylogeny of three pospiviroids from ornamental plants. *Can. J. Plant Pathol.*, **27(4)**: 592-602.
15. **Serra, M.. J.; D. H. Turner and S. M. Freier (1995).** Predicting thermodynamic properties of RNA., *Meth. Enzymol.*, 259: 243-261.
16. **Tamura, K., Dudley, J., Nei, M., and Kumar, S. (2007).** MEGA4: molecular evolutionary genetics analysis (MEGA) software version 4.0. *Mol. Biol. Evol.*, **24**: 1596–1599.
17. **Thompson, J.D., Higgins, D.G., and Gibson, T.J. (1994).** clustalw. Improving the sensitivity of progressive multiple sequence alignment through sequencing weighting, positions-specific gap penalties and weight matrix choice. *Nucleic Acids Res.*, **22:** 4673–4680.
18. **Zuker, M. (1989).** On finding all suboptimal foldings of an RNA molecule. *Science*, **244**: 48–52.